Figure 1. Correlation of PAI-1 mRNA expression with survival of patients with ovarian cancer. Microarray expression data for 2 probe sets representing SERPINE1 (A: 202627_s_at, and B: 202628_s_at) were used to generate Kaplan–Meier survival curves for high expression (defined as cancers with values above the median) or low expression for ovarian cancers. Data were analyzed using GraphPad Prism.

with higher PAI-1 expression showed significantly shorter survival (**Fig. 1**).

PAI-1 expression in ovarian cancer cells

PAI-1 expression was determined in 6 ovarian cancer cell lines established from 2 major histological subtypes, including clear cell and serous subtypes. Immunoblot analysis revealed 2 bands (45 and 40 kDa) of PAI-1 protein in all 6 cell lines (**Fig. 2**). The larger band represented the intact form of PAI-1 and the smaller band represented the cleaved, or inactive, form.[20] These results confirmed that PAI-1 was easily cleaved at its reactive site under physiological conditions. PAI-1 protein expression varied among the individual cell lines, and ES-2 cells showed the highest PAI-1 expression. PAI-1 protein expression in all cell lines was correlated with mRNA levels as determined by quantitative real-time PCR (data not shown).

Knockdown of PAI-1 by siRNA suppresses cell proliferation

To determine the role of PAI-1 in cell growth, small interfering RNA (siRNA)-mediated knockdown of PAI-1 was first examined in ES-2 cells, which show high levels of PAI-1 expression. Three individual siRNA sequences against PAI-1 (#1, #2 and #3) were transfected into ES-2 cells and immunoblotting confirmed
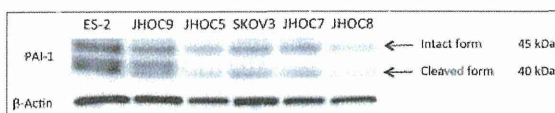

Figure 2. PAI-1 expression in ovarian cancer cell lines. ES-2, JHOC-9, JHOC-5, SKOV3, JHOC-7 and JHOC-8 cells were harvested and whole cell lysates were prepared. Proteins were subjected to immunoblot analysis with antibodies specific for PAI-1 and β-actin. Equal amounts of protein (10 μg) were loaded in each lane.

decreased expression of PAI-1 protein (**Fig. 3A**) compared with control siRNAs (#1 and #2). The percentage of PAI-1 knockdown by PAI-1 siRNAs #1, #2 and #3 was 58%, 77%, and 74%, respectively.

To test whether PAI-1 has tumorigenic activity, the effects of PAI-1 knockdown on cell growth were determined in ES-2 cells. Transfection of ES-2 cells with the 3 PAI-1 siRNAs significantly inhibited proliferation compared with both control siRNAs (#1 and #2) at 72 and 96 h (**Fig. 3B**). Compared with control siRNA #1, the percentage of growth inhibition by PAI-1 siRNAs #1, #2, and #3 at 96 h was 50.6%, 39.2 %, and 47.7%, respectively. Even after 48 h transfection with PAI-1 siRNAs (#1, #2 and #3), cell proliferation was decreased compared with that of control siRNA #2-transfected cells. These results suggest that PAI-1 is involved in cell proliferation.

To determine the mechanisms underlying the antiproliferative effects of PAI-1 siRNA, the cell cycle was evaluated by FACS analysis of ES-2 cells transfected with PAI-1 siRNA. Knockdown of PAI-1 by PAI-1 siRNA #2 arrested the cell cycle at G2/M phase and led to slight accumulation in subG1-like population (**Fig. 3C**). Results from 3 independent experiments showed that PAI-1 siRNA #2 significantly increased the percentage of cells in G2/M phase from $20.1 \pm 1.0\%$ to $35.8 \pm 2.3\%$ and decreased the percentage in S phase from $20.4 \pm 1.0\%$ to $8.6 \pm 1.5\%$, compared with control siRNA #1 (**Fig. 3C**). Together these results suggest that loss of PAI-1 results in G2/M cell cycle arrest.

Increased G2/M arrest has been associated with enhanced apoptosis.[21] To examine the potential effects of PAI-1 siRNA on apoptosis, Annexin V/propidium iodide (PI) staining was employed. PAI-1 knockdown increased the percentage of PI-negative and Annexin-V-positive cells from $2.5 \pm 0.3\%$ (control siRNA #1) to $11.1 \pm 3.8\%$ (**Fig. 3D**). Poly (ADP-ribose) polymerase (PARP) cleavage and caspase 3/7 activation are also typical biochemical characteristics of apoptosis. In ES-2 and JHOC-9 cells treated with individual PAI-1 siRNAs, cleaved PARP (**Fig. 3E**) and caspase 3/7 activity (**Fig. 3F**) were significantly increased compared to control siRNA-treated cells (**Fig. 3E**). These results demonstrate that loss of PAI-1 promotes apoptosis in PAI-1-expressing cells.

PAI-1 was shown to protect cell from Fas-mediated apoptosis,[22] and PAI-1 knockdown is thought to promote extrinsic pathway in which caspase 8 is involved. Contrary to caspase 3 activation, PAI-1 knockdown decreased caspase-8 activation (**Fig. 3G**). Therefore, it is unlikely that extrinsic pathway contributes to the apoptosis in PAI-1-knocked-down ovarian cancer cells.

The intrinsic apoptosis pathway is the primary death program responsive to stress signals such as DNA damages. The central conduit of this pathway is the mitochondrion. Mitochondrial
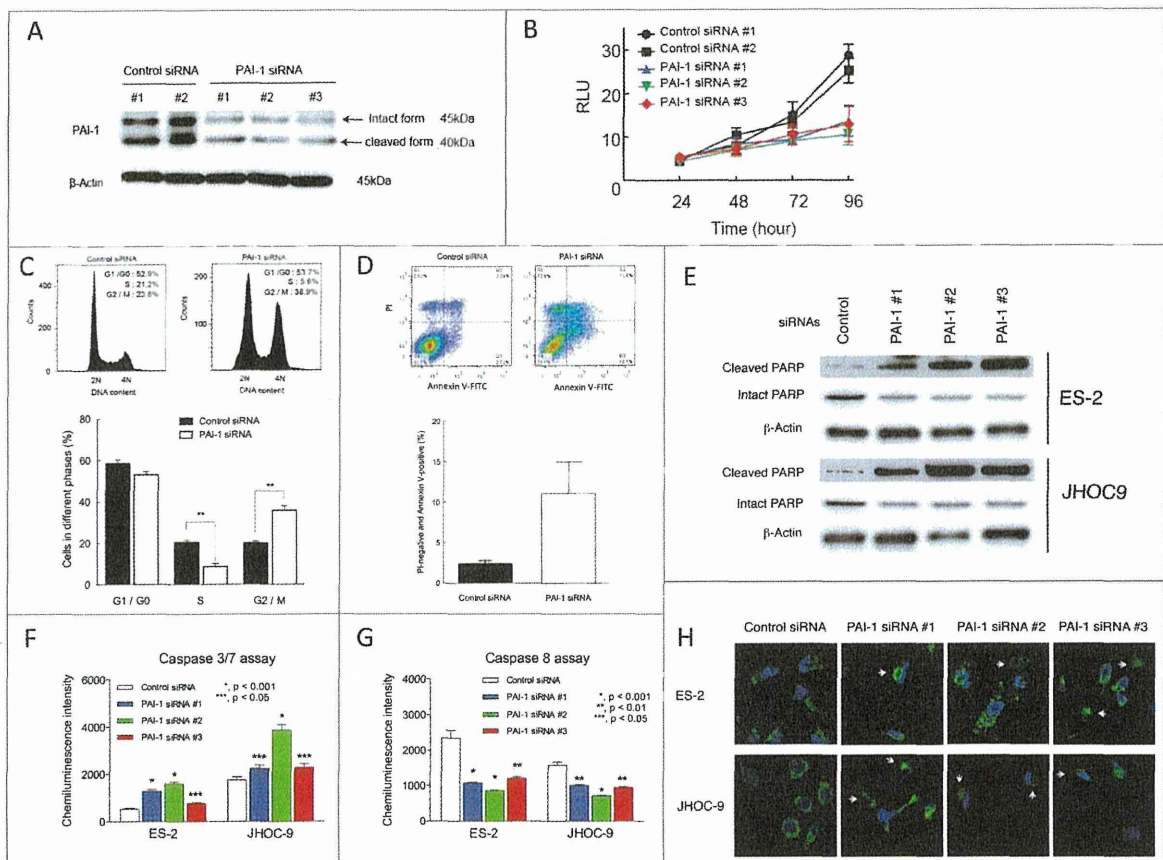
Figure 3. Effect of PAI-1 siRNA on cell viability, cell cycle distribution, and apoptosis in ovarian cancer ES-2 cells. ES-2 cells were transfected with 5 nM control siRNA (#1 and #2) or 5 nM PAI-1 siRNA (#1, #2 and #3) for up to 96 h. (**A**) After 72 h transfection, ES-2 cells were harvested and whole cell lysates were prepared. Proteins were subjected to immunoblot analysis with antibodies specific for PAI-1 and β-actin. Equal amounts of protein (5 μg) were loaded in each lane. (**B**) Cell viability was determined by CellTiter-Glo assay following transfection with siRNA for the indicated periods of time. Values are means ± SD. At 48 h post-transfection, the viability of ES-2 cells transfected with PAI-1 siRNA (#1, #2 and #3) was significantly decreased compared with that of control siRNA (#2) ($P < 0.01$ by Student t test for 2 variables). At 72 and 96 h post-transfection, the viability of ES-2 cells transfected with PAI-1 siRNA (#1, #2 and #3) was significantly decreased compared with cells transfected with control siRNA (#1 and #2). $P < 0.01$ at 72 h; $P < 0.001$ at 96 h by Student t test for 2 variables. (n = 8). (**C**) ES-2 cells were transfected with 5 nM control siRNA #1 or 5 nM PAI-1 siRNA #2 for 72 h. After fixation, cells were stained with PtdIns. Cell cycle distribution was determined by FACS with FlowJo analysis. Representative FACS results of cells transfected with control siRNA (upper left panel) or PAI-1 siRNA (upper right panel) are shown. Cell cycle distribution from 3 independent experiments. Values are means ± SEM. **$P < 0.005$ by Student t test for 2 variables. (**D**) ES-2 cells transfected with 5 nM control siRNA#1 (upper left panel) or 5 nM PAI-1 siRNA #2 (upper right panel) for 72 h. Cells were stained with FITC-conjugated Annexin V and PI, and FACS analysis was performed. Representative FACS results are shown. PI-negative and Annexin-V-positive cells from 3 experiments. Values are means ± SE. (**E**) ES-2 or JHOC-9 cells transfected with 5 nM control siRNA #2 or PAI-1 siRNAs (#1, #2 and #3) for 72 h were harvested and whole cell lysates were prepared. Proteins were subjected to immunoblot analysis with antibodies specific for cleaved PARP, intact PARP and β-actin. Equal amounts of protein (5 μg) were loaded in each lane. (F and G) ES-2 or JHOC-9 cells were transfected with the indicated siRNAs. After 72 h, activation of caspase 3/7 or caspase 8 was assessed by Caspase-Glo 3/7 or Caspase-Glo8, respectively. Values are means ± SE (n = 4). P values were determined by Student t test, control siRNA vs. PAI-1 siRNA. (**H**) ES-2 or JHOC-9 cells were transfected with the indicated siRNAs. After 72 h, cells were fixed and stained with cytochrome c antibody (green) and Hoechst33342 (blue). Imaging was performed by confocal microscopy. White allows show cells with cytochrome c released from mitochondria to cytoplasm.

damage results in cytochrome c release from mitochondria and formation of apoptosome, leading to activation of caspase 9 and subsequent activation of caspase 3/7.[23,24] Confocal microscopy revealed that the tubular pattern of cytochrome c staining became diffuse in cells treated with individual PAI-1 siRNAs, indicating cytochrome c release from mitochondria (**Fig. 3H**). Therefore, PAI-1-knockdown is suggested to facilitate the intrinsic pathway of apoptosis by damaging mitochondria.

Pharmacological inhibition of PAI-1 by TM5275 decreases cell proliferation of ovarian cancer cells

TM5275 is a small molecule inhibitor specific for PAI-1 (**Fig. 4A**) that has been developed as a therapeutic reagent for PAI-1-associated diseases.[17,18] We investigated its potential as a therapeutic reagent for targeting cell proliferation in ovarian cancer. Ovarian cancer cells were treated with various concentrations of TM5275. Cell viability at 72 h treatment was decreased with
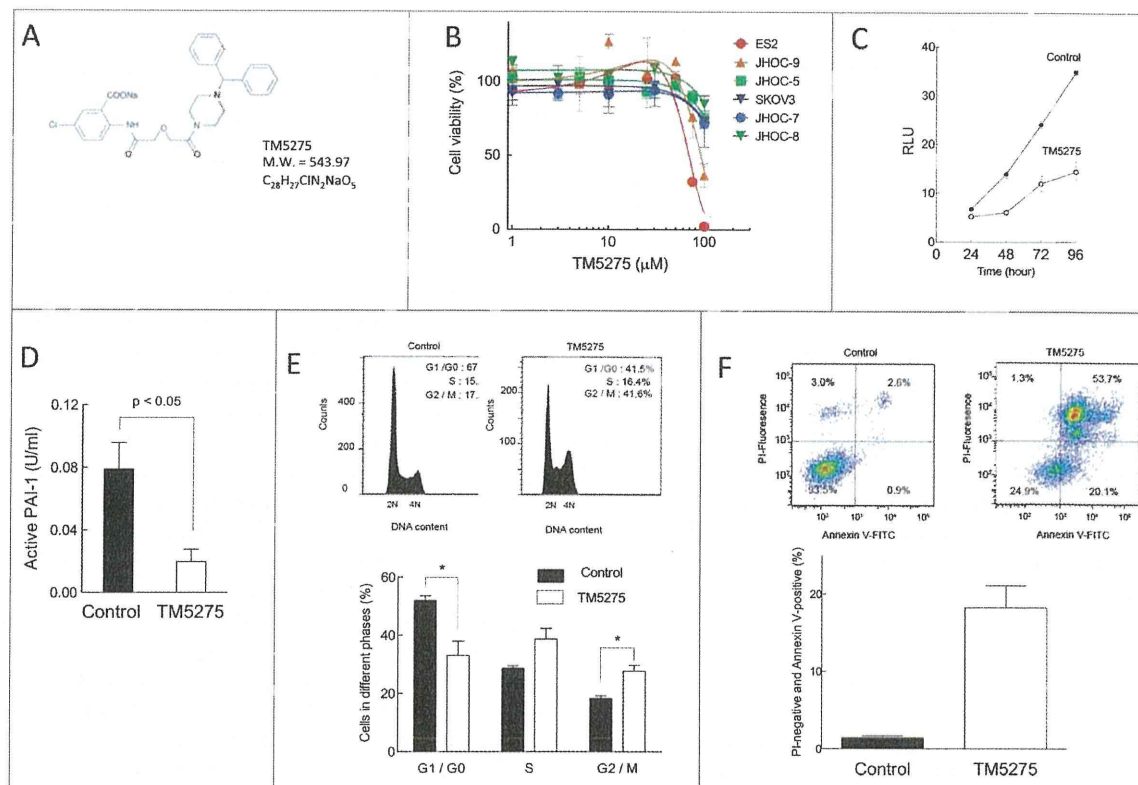
Figure 4. Effects of TM5275 on cell viability, cell cycle distribution and apoptosis induction in ovarian clear cell adenocarcinoma cells. (**A**) Chemical structure of TM5275. (**B**) ES-2, JHOP-9, JHOC-5, SKOV3, JHOC-7 and JHOC-8 cells were treated with the indicated concentrations of TM5275 for 72 h. Cell viability was determined by CellTiter-Glo assay in 3 experiments. Values are means $\pm$ SD. IC50 in individual cell lines is shown in **Table 1**. (**C**) ES2 were treated with DMSO (control) or 100 μM TM5275 for the indicated periods. Cell growth was determined by CellTiter-Glo assay ($n = 3$). (**D**) After TM5275 treatment for 96 h, cell culture media of ES2 cells were harvested. Active PAI-1 amounts were determined by active human PAI-1 functional assay ELISA kit ($n = 4$). (**E**) ES-2 cells were treated with DMSO (upper left panel) or 100 μM TM5275 (upper right panel) for 24 h. After fixation, cells were stained with PI. Cell cycle distribution was determined by FACS with FlowJo analysis. Representative FACS results are shown. Cell cycle distribution from 3 independent experiments. Values are means $\pm$ SE. *$P < 0.05$ by Student t test for 2 variables ($n = 3$). (**F**) ES-2 cells were treated with DMSO (upper left panel) or 100 μM TM5275 (upper right panel) for 24 h. Cells were stained with FITC-conjugated Annexin V and PI, and FACS analysis was performed. Representative FACS results are shown. PI-negative and Annexin-V-positive cells from 3 experiments. Values are means $\pm$ SE. *$P < 0.005$ by Student t test for 2 variables ($n = 3$).

70–100 μM TM5275 in ES-2 and JHOC-9 cells, whereas other cell lines were relatively insensitive to TM5275 treatment (**Fig. 4B**). The IC50 values for TM5275 in ovarian cancer cell lines are shown in **Table 1**. Further, cell growth was measured at the indicated time points after TM5275 treatment. From 48 h up to 96 h, cell growth was suppressed with 100 μM TM5275 (**Fig. 4C**). Furthermore, active PAI-1 in cell culture media was significantly decreased in cells treated with 100 μM TM5275 compared to control treatment, confirming TM5275 effectiveness for PAI-1 inhibition (**Fig. 4D**). These results suggest that ovarian cancer cells with high expression of PAI-1, such as ES-2 and JHOC-9, are prone to growth inhibition by TM5275. Taken together, pharmacological inhibition of PAI-1 by TM5275 is suggested to exert anti-proliferative effects in ovarian cancer with high PAI-1 expression.

To determine the effects of TM5275 on cell cycle progression of ES-2 cells, cells were treated with or without TM5275 for 24 h and cell cycle distribution was analyzed. Compared with vehicle treatment, TM5275 treatment significantly decreased the percentage of cells in G0/G1 ($52.0 \pm 1.5\%$ to $33.0 \pm 4.9\%$) and increased the percentage in G2/M ($18.3 \pm 0.8\%$ to $27.7 \pm 2.0\%$) (**Fig. 4E**). Moreover, cells treated with TM5275 showed a significant increase in the percentage of apoptotic cells (**Fig. 4F**). These results demonstrated that pharmacological inhibition of PAI-1 induced a G2/M cell cycle arrest and promoted apoptotic cell death in ovarian cancer cells in accordance with the knockdown of PAI-1 by siRNAs.

PAI-1 expression in major histological subtypes of ovarian carcinoma

Expression of PAI-1 protein was evaluated in 27 ovarian cancer patients by immunohistochemical analysis of a tissue array. Consistent with previous reports on PAI-1 staining,[10] strong staining of PAI-1 was observed in the cytoplasm of cancer cells of

147

Table 1. IC50 values of TM5275 for cell viability of ovarian carcinoma cell lines.

Cell lines	IC50 (μM)
ES-2	67
JHOC-9	92.5
JHOC-5	>100
SKOV3	>100
JHOC-7	>100
JHOC-8	>100

Table 2. The number of PAI-1-positive and -negative samples in individual histological subtypes of ovarian cancer. PAI-1-positive expression is significantly associated with clear cell subtype ($P < 0.05$ in χ^2 test).

Histological subtype	PAI-1-positive	PAI-1-negative
Clear cell (%)	13	1
Serous (%)	4	9

the clear cell subtype (**Fig. 5**). In the PAI-1-positive serous subtype specimen, stromal cells were PAI-1-positive to a lesser extent relative to cancer cells (**Fig. 5**). PAI-1-positive staining was detected in 92.8% (13 out of 14) of the clear cell subtype and 30.7% (4 out of 13) of the serous subtype (**Table 2**). These findings suggest that clear cell subtype may be prone to PAI-1-positive expression relative to serous subtypes. Thereby, PAI-1-targeted therapy might be more appropriate for clear cell ovary carcinoma compared with the serous subtype.

Discussion

Multiple studies have demonstrated a considerable association of PAI-1 with cancer, and PAI-1 has been emerging as a therapeutic target for cancer. Our study demonstrated for the first
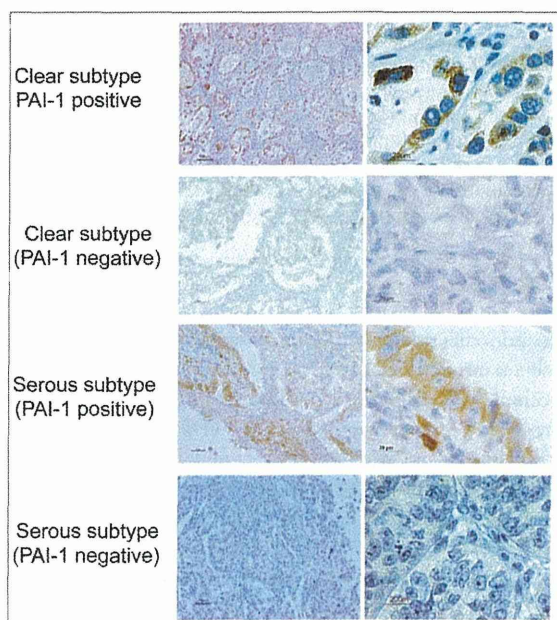

Figure 5. PAI-1 expression in different histological subtypes of human ovarian carcinoma. Cancer tissues were stained with PAI-1 antibody. Representative examples of PA1-1-positive and -negative immunostaining in tissues of ovarian clear cell and serous adenocarcinoma, respectively (original magnification: left panels, 200×; right panels, 1,000×). Scale bars represent 50 or 100 μm (left panels), and 20 μm (right panels).

time that genetic and pharmacological inhibition of PAI-1 suppresses cell proliferation of ovarian cancer and supports the potential of PAI-1-targeted pharmacotherapeutics for ovarian cancer. Our findings also suggest that the small molecule PAI-1 inhibitor TM5275 represents a novel class of anti-tumor agents.

A number of studies have shown that high levels of PAI-1 expression are predictive of poor prognosis in several types of human cancer.[4-9,25,26] In our study, a database search demonstrated that PAI-1 was a significant biomarker of poor prognosis in patients with ovarian cancer (**Fig. 1**). In addition, we confirmed PAI-1 expression in 6 individual ovarian cancer cell lines (**Fig. 2**). On the other hand, a high concentration of plasma tPA was also reported as an independent marker for poor prognosis in patients with ovarian cancer.[27] Previous studies also showed that high PAI-1-tPA complex levels are associated with shorter progression-free and overall survival in breast cancer.[28,29] Considering the pathobiological role of the plasminogen activation system in cancer invasion and metastasis,[30,31] PAI-1 and tPA may coordinately regulate the progression of ovarian cancer.

In our study, genetic and pharmacological inhibition of PAI-1 led to suppression of cell proliferation, G2/M cell cycle arrest, and apoptosis in ovarian cancer cells (**Figs. 3 and 4**). Reciprocally, enforced expression of PAI-1 was shown to promote cell growth.[32] Together these data suggest that PAI-1 serves as a proliferative and/or an antiapoptotic molecule in ovarian cancer.

Modulation of cell cycle arrest in G2/M phase has been emerging as a focus of research in laboratory and clinical cancer studies.[33] Our studies suggest the potential of novel roles for PAI-1 in the progression and/or checkpoint of G2/M phase, although the molecular mechanism remains unknown.

A PAI-1 inhibitor TM5275 prevents PAI-1 interaction with the LDL receptor-related protein 1(LRP1).[18] As LRP1 has been shown to promote anti-apoptotic signaling, stimulatory effects of TM5275 on apoptosis of ovarian cancer (**Fig. 4**) might result from inhibiting PAI-1 interaction with LRP1. PAI-1 might exert a protective effect against cancer cell apoptosis.

In vitro inhibitory activity of TM5275 has been measured by tPA-dependent hydrolysis of peptide substrate, revealing the IC50 value (6.95 μM).[17] This concentration was substantially not sufficient to suppress cell growth of ovarian cancer (**Fig. 4**). This diversity may be due to the high degree of protein binding (>99.9%) or the *Ki* value of TM5275 for specific PAI-1-interacting protein(s) involved in cell growth or insufficient delivery to cells.

In vivo pharmacokinetics and toxicity of TM5275 have been evaluated not only in rodents but also in nonhuman primates, showing *Cmax* value in orally-administrated rats (34 μM) and no

significant toxic effects.[17] In the present studies, 70 μM TM5275 in ES-2 cells had an inhibitory effect on cell growth (Fig. 4), probably raising the potential of TM5275 therapeutic efficacy for ovarian cancer treatment. We have been also developing its derivative TM5441 as a therapeutic reagent for PAI-1-associated diseases, certainly suggesting that these PAI-1 inhibitors may eventually prove to be useful as novel drugs.[34]

Venous thromboembolism is a common complication of malignant disease, and the association between cancer and thrombosis is well established.[35-37] Ovarian cancer is associated with high rates of venous thromboembolism.[38] Up-regulation of PAI-1 could be involved in the clinical features and pathogenesis of both medical conditions. Therefore, a molecular therapy targeting PAI-1 may effectively improve prognosis of cancer patients.

Clear cell carcinoma of the ovary is the histologic subtype that is most frequently associated with an unusual high rate of venous thromboembolism.[39] This clinical feature could be associated with PAI-1 up-regulation in clear cell carcinoma of the ovary (Fig. 5 and Table 2). In addition, ES-2 cells established from the clear cell subtype showed higher expression of PAI-1 compared with those of serous subtype (SKOV3 cells) (Fig. 2). Recent studies showed that significant amplification of MET oncogene is commonly observed in ovarian clear cell carcinoma.[40,41] As that oncogene has been implicated in blood coagulation and cancers that are accompanied with PAI-1 up-regulation,[37] MET-driven PAI-1 could be closely associated with the progression and complications of clear cell carcinoma of the ovary. Thus, inhibiting PAI-1 might be effective in treating ovarian clear cell carcinoma.

Taken together, our results suggest that PAI-1 contributes to cell proliferation of ovarian cancer and might be involved in G2/M cell cycle checkpoint or progression. Considering PAI-1 pathobiology, its inhibitors such as TM5275 and its derivatives may represent a novel class of anti-tumor agents for ovarian cancer. In particular, PAI-1-targeted pharmacotherapy may be preferentially effective against the clear cell subtype of ovarian cancer.

Materials and Methods

Materials

The ES-2 and SKOV3 human ovarian cancer cell lines were obtained from American Type Culture Collection (ATCC). Other ovarian cancer cells (JHOC-5, JHOC-7, JHOC-8 and JHOC-9) were kindly provided by Dr. Katsutoshi Oda (University of Tokyo, Tokyo, Japan). Horseradish-peroxidase-conjugated antibodies for mouse and rabbit IgG were from Santa Cruz Biotechnology. Cleaved PARP antibody was from Cell Signaling Technology. β-Actin antibody was from Sigma-Aldrich. Individual PAI-1 antibodies for immunoblotting and immunohistochemistry were from Abcam and Leica Biosystems, respectively. Three individual siRNA oligonucleotides directed against human PAI-1 (#1, S10013; #2, S10014; and #3, S10015) and 2 control siRNAs (#1, 4390843; and #2, 4390846) were purchased from Life Technologies. CellTiter-Glo Luminescent Cell Viability Assay kit, Caspase-Glo 3/7, and Caspase-Glo 8 were from

Promega. Cytochrome c antibody was from BD Biosciences. Active human PAI-1 functional assay ELISA kit was from Molecular Innovations. TM5275, 5-chloro-2-((2-(4-(diphenylmethyl) piperazin-1-yl)-2-oxoethoxy) acetyl) amino) benzoate[17,18] has been established as a PAI-1 inhibitor (Division of Molecular Medicine and Therapy, United Centers for Advanced Research and Translational Medicine, Tohoku University Graduate School of Medicine, Sendai, Japan).

Clinical studies

For examining the association between SERPINE1 expression and outcome (overall survival and progression free survival), patients with ovarian cancer (n = 228) were selected from the Australian Ovarian Cancer Study (AOCS), a population-based, multicenter translational study that comprised a prospective collection of bio-specimens and clinical and epidemiological data from patients with primary epithelial ovarian, primary peritoneal and fallopian tube cancer diagnosed between 2001 and 2005. All patients had provided consent using a protocol approved by human research ethics committees at multiple participating clinical and research centers. Methods for RNA extraction and expression profiling were previously reported.[19]

Cell culture

Ovarian cancer cells were cultured as monolayer cultures in Dulbecco's Modified Eagle's Medium supplemented with 10% fetal bovine serum. Cells were maintained at <80% confluence under standard incubator conditions (humidified atmosphere, 95% air, 5% CO_2, 37°C).

Immunoblotting

Cells were washed 3 times with PBS containing 10 mM EDTA and then lysed using Laemmli buffer. Protein samples (5 or 10 μg) were subjected to SDS-PAGE (4–20% gradient gels). Proteins were electrophoretically transferred to nitrocellulose membranes, blocked with PBS/0.1% Tween 20 (PBS-T) containing 5% nonfat dried milk, washed with PBS-T, and incubated with antibodies to β-actin (1 in 40,000 dilution), PAI-1 (1 in 500 dilution), PARP (1 in 2,000 dilution), or cleaved PARP (1 in 1,000 dilution) in PBS-T containing 5% nonfat dried milk. The blots were washed with PBS-T and incubated with secondary antibody conjugated with horseradish peroxidase in PBS-T containing 5% nonfat dried milk. Detection was performed using enhanced chemiluminescence reagents, and the quantification of the chemiluminescent signals was performed with a digital imaging system (VersaDoc; Bio-Rad).

Transfection with siRNAs

Cells (1 × 10^5/60-mm dish or 1–2 × 10^3/96-well plate) were transfected with 5 nM double-stranded PAI-1 siRNAs using Lipofectamine RNAi Max Transfection Reagent (Life Technologies) according to the manufacturer's instructions.

Cell viability assay

Cell viability was assessed with the CellTiter-Glo Luminescent Cell Viability Assay. Cells were seeded on 96-well plates at a

density of 1–2 × 10^3/well. After treatment with siRNA TM5275, 80 μl CellTiter-Glo reagent was added to each well, and then plate contents were mixed on an orbital shaker. Luminescence was quantified on a standard luminometer.

Cell cycle analysis

ES-2 cells (1 × 10^6/100-mm dish) were subjected to the appropriate treatment. The cells were trypsinized and fixed with ice-cold 70% ethanol overnight. Fixed cells were washed with PBS and stained with 50 μg/ml propidium iodide (PI) in the presence of 100 μg/ml RNase. Cellular fluorescence was quantitated using the FL3 channel of a flow cytometer (FACSCanto II, BD Systems). The cell cycle distribution was determined using FlowJo software (Tree Star Inc..).

Annexin V staining

ES-2 cells (1 × 10^6/100-mm dish) were subjected to the appropriate treatment. The cells were trypsinized, washed with PBS, and stained with AlexaFluor-488-conjugated Annexin V and PI from the Dead Cell Apoptosis Kit (Life Technologies). The stained cells were analyzed using a flow cytometer (BD Systems).

Caspase assay

Caspase activation was determined by Caspase-Glo 3/7 or Caspase-Glo 8 assay kits.[42] Cells, seeded on 96-well plates at a density of 2 × 10^3/well, were transfected with siRNAs. After 72 h, 80 μl of individual Caspase-Glo reagent was added. Following 0.5 h incubation at room temperature, samples were read on a microplate luminometer.

Immunocytochemistry

Cytochrome c staining was performed by the method as described in Kitatani et al.[43] Cells, growing on glass coverslips, were fixed for 10 min at room temperature with 4% formaldehyde in PBS and washed with PBS. Next, cells were treated for 10 min with 0.1% TritonX-100, washed with PBS, and blocked for 1 hour with PBS containing 2% human serum. Cells were incubated with cytochrome c antibody in PBS containing 2% human serum over night. After washing with PBS, cells were further incubated with Alexa488-conjugated anti-IgG antibody and Hoech33342 in PBS containing 2% human serum for 1 h. Confocal laser microscopy was performed using an LSM780 confocal microscope (Carl Zeiss, NY).

PAI-1 activity assay

ES-2 cells (5 × 10^4), grown on 60 mm-dishes, were treated with DMSO (control) or 100 μM TM5275 for 96 h. Cell culture media were harvested, and active PAI-1 was determined by active human PAI-1 functional assay ELISA kit according to the manufacturer's protocol.

Human tissue samples

A total of 27 human tissue samples were obtained from the Surgical Pathology Archives of Obstetrics and Gynecology Department of Tohoku University Hospital (Sendai, Japan). Tissues were fixed in buffered-formalin and embedded in paraffin, followed by staining with hematoxylin and eosin, or PAI-1. This study was approved by the Ethics Committee at the Tohoku University Graduate School of Medicine (Sendai, Japan).

Immunohistochemistry

After deparaffinization, tumor tissues were stained with PAI-1 antibody. Immunohistochemical analysis was performed with the streptavidin–biotin amplification method using a Histofine kit (Nichirei). The immunohistochemical staining of tumor tissues for PAI-1 was evaluated and scored as follows: negative, no or weak staining: <10% of cells; or positive, moderate to strong staining: >10% of cells. Two independent, blind observers evaluated immunostained sections (5 fields/section).

Statistical analysis

Statistical analyses were performed using GraphPad Prism (Graphpad Software Inc..). Comparisons of continuous variables were assessed using the Student t test for 2 variables. All p values were 2-sided and derived using Fisher's exact test or the χ^2 test. $P < 0.05$ was considered statistically significant.

References

1. Siegel R, Naishadham D, Jemal A. Cancer statistics, 2012. CA Cancer J Clin 2012; 62:10-29; PMID:22237781; http://dx.doi.org/10.3322/caac.20138
2. Kohler HP, Grant PJ. Plasminogen-activator inhibitor type 1 and coronary artery disease. N Engl J Med 2000; 342:1792-801; PMID:10853003; http://dx.doi.org/10.1056/NEJM200006153422419
3. Schuliga M, Westall G, Xia Y, Stewart AG. The plasminogen activation system: new targets in lung inflammation and remodeling. Curr Opin Pharmacol 2013; 13:386-93; PMID:23735578; http://dx.doi.org/10.1016/j.coph.2013.05.014
4. Allgayer H, Heiss MM, Schildberg FW. Prognostic factors in gastric cancer. Br J Surg 1997; 84:1651-64; PMID:9448610; http://dx.doi.org/10.1002/bjs.1800841206
5. Berger DH. Plasmin/plasminogen system in colorectal cancer. World J Surg 2002; 26:767-71; PMID:11965442; http://dx.doi.org/10.1007/s00268-002-4050-8
6. Offersen BV, Alsner J, Ege Olsen K, Riisbro R, Brunner N, Sorensen FB, Sorensen BS, Schlemmer BO, Overgaard J. A comparison among HER2, TP53, PAI-1, angiogenesis, and proliferation activity as prognostic variables in tumours from 408 patients diagnosed with

early breast cancer. Acta Oncol 2008; 47:618-32; PMID:18465330; http://dx.doi.org/10.1080/02841860801958295

7. Foekens JA, Look MP, Peters HA, van Putten WL, Portengen H, Klijn JG. Urokinase-type plasminogen activator and its inhibitor PAI-1: predictors of poor response to tamoxifen treatment in recurrent breast cancer. J Natl Cancer Inst 1995; 87:751-6; PMID:7563153; http://dx.doi.org/10.1093/jnci/87.10.751

8. Harbeck N, Thomssen C, Berger U, Ulm K, Kates RE, Hofler H, Janicke F, Graeff H, Schmitt M. Invasion marker PAI-1 remains a strong prognostic factor after long-term follow-up both for primary breast cancer and following first relapse. Breast Cancer Res Treat 1999; 54:147-57; PMID:10424405; http://dx.doi.org/10.1023/A:1006118828278

9. Zekanowska E, Cieslinski K, Rose D. [Plasminogen activator inhibitor type 1 (PAI-1) in blood and tissue extracts of patients with non-small cell lung cancer]. Pneumonol Alergol Pol 2004; 72:409-14; PMID:16021996

10. Zubac DP, Wentzel-Larsen T, Seidal T, Bostad L. Type 1 plasminogen activator inhibitor (PAI-1) in clear cell renal cell carcinoma (CCRCC) and its impact on angiogenesis, progression and patient survival after radical nephrectomy. BMC Urol 2010; 10:20; PMID:21129210; http://dx.doi.org/10.1186/1471-2490-10-20

11. Chambers SK, Ivins CM, Carcangiu ML. Plasminogen activator inhibitor-1 is an independent poor prognostic factor for survival in advanced stage epithelial ovarian cancer patients. Int J Cancer 1998; 79:449-54; PMID:9761111; http://dx.doi.org/10.1002/(SICI)1097-0215(19981023)79:5%3c449::AID-IJC1%3e3.0.CO;2-0

12. Kuhn W, Schmalfeldt B, Reuning U, Pache L, Berger U, Ulm K, Harbeck N, Spathe K, Dettmar P, Hofler H, et al. Prognostic significance of urokinase (uPA) and its inhibitor PAI-1 for survival in advanced ovarian carcinoma stage FIGO IIIc. Br J Cancer 1999; 79:1746-51; PMID:10206287; http://dx.doi.org/10.1038/sj.bjc.6690278

13. Alberti C, Pinciroli P, Valeri B, Ferri R, Ditto A, Umezawa K, Sensi M, Canevari S, Tomassetti A. Ligand-dependent EGFR activation induces the co-expression of IL-6 and PAI-1 via the NFkB pathway in advanced-stage epithelial ovarian cancer. Oncogene 2012; 31:4139-49; PMID:22158046; http://dx.doi.org/10.1038/onc.2011.572

14. Balsara RD, Ploplis VA. Plasminogen activator inhibitor-1: the double-edged sword in apoptosis. Thromb Haemost 2008; 100:1029-36; PMID:19132226

15. Webb DJ, Thomas KS, Gonias SL. Plasminogen activator inhibitor 1 functions as a urokinase response modifier at the level of cell signaling and thereby promotes MCF-7 cell growth. J Cell Biol 2001; 152:741-52; PMID:11266465; http://dx.doi.org/10.1083/jcb.152.4.741

16. Fang H, Placencio VR, DeClerck YA. Protumorigenic activity of plasminogen activator inhibitor-1 through an antiapoptotic function. J Natl Cancer Inst 2012; 104:1470-84; PMID:22984202; http://dx.doi.org/10.1093/jnci/djs377

17. Izuhara Y, Yamaoka N, Kodama H, Dan T, Takizawa S, Hirayama N, Meguro K, van Ypersele de Strihou C, Miyata T. A novel inhibitor of plasminogen activator inhibitor-1 provides antithrombotic benefits devoid of bleeding effect in nonhuman primates. J Cereb Blood Flow Metab 2010; 30:904-12; PMID:20087372; http://dx.doi.org/10.1038/jcbfm.2009.272

18. Ichimura A, Matsumoto S, Suzuki S, Dan T, Yamaki S, Sato Y, Kiyomoto H, Ishii N, Okada K, Matsuo O, et al. A small molecule inhibitor to plasminogen activator inhibitor 1 inhibits macrophage migration. Arterioscler Thromb Vasc Biol 2013; 33:935-42; PMID:23471233; http://dx.doi.org/10.1161/ATVBAHA.113.301224

19. Tothill RW, Tinker AV, George J, Brown R, Fox SB, Lade S, Johnson DS, Trivett MK, Etemadmoghadam D, Locandro B, et al. Novel molecular subtypes of serous and endometrioid ovarian cancer linked to clinical outcome. Clin Cancer Res 2008; 14:5198-208; PMID:18698038; http://dx.doi.org/10.1158/1078-0432.CCR-08-0196

20. Wu K, Urano T, Ihara H, Takada Y, Fujie M, Shikimori M, Hashimoto K, Takada A. The cleavage and inactivation of plasminogen activator inhibitor type 1 by neutrophil elastase: the evaluation of its physiologic relevance in fibrinolysis. Blood 1995; 86:1056-61; PMID:7620159

21. DiPaola RS. To arrest or not to G(2)-M Cell-cycle arrest: commentary re: A. K. Tyagi et al., Silibinin strongly synergizes human prostate carcinoma DU145 cells to doxorubicin-induced growth inhibition, G(2)-M arrest, and apoptosis. Clin Cancer Res 2002; 8:3512-9 Clin Cancer Res 2002; 8:3311-4; PMID:12429616

22. Bajou K, Peng H, Laug WE, Maillard C, Noel A, Foidart JM, Martial JA, DeClerck YA. Plasminogen activator inhibitor-1 protects endothelial cells from FasL-mediated apoptosis. Cancer Cell 2008; 14:324-34; PMID:18835034; http://dx.doi.org/10.1016/j.ccr.2008.08.012

23. Li P, Nijhawan D, Budihardjo I, Srinivasula SM, Ahmad M, Alnemri ES, Wang X. Cytochrome c and dATP-dependent formation of Apaf-1/caspase-9 complex initiates an apoptotic protease cascade. Cell 1997; 91:479-89; PMID:9390557; http://dx.doi.org/10.1016/S0092-8674(00)80434-1

24. Goldstein JC, Waterhouse NJ, Juin P, Evan GI, Green DR. The coordinate release of cytochrome c during apoptosis is rapid, complete and kinetically invariant. Nat Cell Biol 2000; 2:156-62; PMID:10707086; http://dx.doi.org/10.1038/35004029

25. Chambers SK, Ivins CM, Carcangiu ML. Plasminogen activator inhibitor-1 is an independent poor prognostic factor for survival in advanced stage epithelial ovarian cancer patients. Int J Cancer 1998; 79:449-54; PMID:9761111; http://dx.doi.org/10.1002/(SICI)1097-0215(19981023)79:5%3c449::AID-IJC1%3e3.0.CO;2-0

26. Kuhn W, Schmalfeldt B, Reuning U, Pache L, Berger U, Ulm K, Harbeck N, Spathe K, Dettmar P, Hofler H, et al. Prognostic significance of urokinase (uPA) and its inhibitor PAI-1 for survival in advanced ovarian carcinoma stage FIGO IIIc. Br J Cancer 1999; 79:1746-51; PMID:10206287; http://dx.doi.org/10.1038/sj.bjc.6690278

27. Borgfeldt C, Bendahl P-O, Fernö M, Casslén B. High preoperative plasma concentration of tissue plasminogen activator (tPA) is an independent marker for shorter overall survival in patients with ovarian cancer. Gynecol Oncol 2003; 91:112-7; PMID:14529669; http://dx.doi.org/10.1016/S0090-8258(03)00493-1

28. de Witte JH, Sweep CG, Klijn JG, Grebenschikov N, Peters HA, Look MP, van Tienoven TH, Heuvel JJ, Bolt-De Vries J, Benraad TJ, et al. Prognostic value of tissue-type plasminogen activator (tPA) and its complex with the type-1 inhibitor (PAI-1) in breast cancer. Br J Cancer 1999; 80:286-94; PMID:10390010; http://dx.doi.org/10.1038/sj.bjc.6690353

29. Raigoso P, Junco A, Andicoechea A, Gonzalez A, Garcia-Muniz JL, Allende MT, Garcia-Moran M, Vizoso F. Tissue-type plasminogen activator (tPA) content in colorectal cancer and in surrounding mucosa: relationship with clinicopathologic parameters and prognostic significance. Int J Biol Markers 2000; 15:44-50; PMID:10763140

30. Dass K, Ahmad A, Azmi AS, Sarkar SH, Sarkar FH. Evolving role of uPA/uPAR system in human cancers.

Cancer Treat Rev 2008; 34:122-36; PMID:18162327; http://dx.doi.org/10.1016/j.ctrv.2007.10.005

31. Andreasen PA, Egelund R, Petersen HH. The plasminogen activation system in tumor growth, invasion, and metastasis. Cell Mol Life Sci 2000; 57:25-40; PMID:10949579; http://dx.doi.org/10.1007/s000180050497

32. Zhang W, Ling D, Tan J, Zhang J, Li L. Expression of urokinase plasminogen activator and plasminogen activator inhibitor type-1 in ovarian cancer and its clinical significance. Oncol Rep 2013; 29:637-45; PMID:23174953

33. DiPaola RS. To arrest or not to G(2)-M Cell-cycle arrest: commentary re: A. K. Tyagi et al., Silibinin strongly synergizes human prostate carcinoma DU145 cells to doxorubicin-induced growth inhibition, G(2)-M arrest, and apoptosis. Clin Cancer Res 2002; 8:3512-9 Clin Cancer Res 2002; 8:3311-4; PMID:12429616

34. Boe AE, Eren M, Murphy SB, Kamide CE, Ichimura A, Terry D, McAnally D, Smith LH, Miyata T, Vaughan DE. Plasminogen activator inhibitor-1 antagonist TM5441 attenuates Nomega-nitro-L-arginine methyl ester-induced hypertension and vascular senescence. Circulation 2013; 128:2318-24; PMID:24092817; http://dx.doi.org/10.1161/CIRCULATIONAHA.113.003192

35. Lee AY, Levine MN. Venous thromboembolism and cancer: risks and outcomes. Circulation 2003; 107: I17-21; PMID:12814981

36. Baron JA, Gridley G, Weiderpass E, Nyren O, Linet M. Venous thromboembolism and cancer. Lancet 1998; 351:1077-80; PMID:9660575; http://dx.doi.org/10.1016/S0140-6736(97)10018-6

37. Boccaccio C, Sabatino G, Medico E, Girolami F, Follenzi A, Reato G, Sottile A, Naldini L, Comoglio PM. The MET oncogene drives a genetic programme linking cancer to haemostasis. Nature 2005; 434:396-400; PMID:15772665; http://dx.doi.org/10.1038/nature03357

38. Rickles FR. Cancer and thrombosis in women - molecular mechanisms. Thromb Res 2009; 123(Suppl 2): S16-20; PMID:19217469; http://dx.doi.org/10.1016/S0049-3848(09)70004-0

39. Duska LR, Garrett L, Henretta M, Ferriss JS, Lee L, Horowitz N. When 'never-events' occur despite adherence to clinical guidelines: the case of venous thromboembolism in clear cell cancer of the ovary compared with other epithelial histologic subtypes. Gynecol Oncol 2010; 116:374-7; PMID:19922988; http://dx.doi.org/10.1016/j.ygyno.2009.10.069

40. Yamamoto S, Tsuda H, Miyai K, Takano M, Tamai S, Matsubara O. Gene amplification and protein overexpression of MET are common events in ovarian clear-cell adenocarcinoma: their roles in tumor progression and prognostication of the patient. Mod Pathol 2011; 24:1146-55; PMID:21478826; http://dx.doi.org/10.1038/modpathol.2011.70

41. Yamashita Y, Akatsuka S, Shinjo K, Yatabe Y, Kobayashi H, Seko H, Kajiyama H, Kikkawa F, Takahashi T, Toyokuni S. Met is the most frequently amplified gene in endometriosis-associated ovarian clear cell adenocarcinoma and correlates with worsened prognosis. PLoS One 2013; 8:e57724; PMID:23469222; http://dx.doi.org/10.1371/journal.pone.0057724

42. Liu JJ, Wang W, Dicker DT, El-Deiry WS. Bioluminescent imaging of TRAIL-induced apoptosis through detection of caspase activation following cleavage of DEVD-aminoluciferin. Cancer Biol Ther 2005; 4:885-92; PMID:16177559; http://dx.doi.org/10.4161/cbt.4.8.2133

43. Kitatani K, Idkowiak-Baldys J, Bielawski J, Taha TA, Jenkins RW, Senkal CE, Ogretmen B, Obeid LM, Hannun YA. Protein kinase C-induced activation of a ceramide/protein phosphatase 1 pathway leading to dephosphorylation of p38 MAPK. J Biol Chem 2006; 281:36793-802; PMID:17030510; http://dx.doi.org/10.1074/jbc.M608137200

RESEARCH ARTICLE

Plasminogen Activator Inhibitor-1 Antagonist TM5484 Attenuates Demyelination and Axonal Degeneration in a Mice Model of Multiple Sclerosis

Nicolas Pelisch[1]*, Takashi Dan[1], Atsuhiko Ichimura[1], Hiroki Sekiguchi[1], Douglas E. Vaughan[2], Charles van Ypersele de Strihou[3], Toshio Miyata[1]

1 Department of Molecular Medicine and Therapy, United Centers for Advanced Research and Translational Medicine, Tohoku University Graduate School of Medicine, Sendai, Miyagi, Japan, 2 Department of Medicine, Northwestern University Feinberg School of Medicine, Chicago, Illinois, United States of America, 3 Service de Nephrologie, Cliniques Universitaires Saint Luc, Brussels, Belgium

* n.pelisch@med.tohoku.ac.jp

Abstract

Multiple sclerosis (MS) is characterized by inflammatory demyelination and deposition of fibrinogen in the central nervous system (CNS). Elevated levels of a critical inhibitor of the mammalian fibrinolitic system, plasminogen activator inhibitor 1 (PAI-1) have been demonstrated in human and animal models of MS. In experimental studies that resemble neuroinflammatory disease, PAI-1 deficient mice display preserved neurological structure and function compared to wild type mice, suggesting a link between the fibrinolytic pathway and MS. We previously identified a series of PAI-1 inhibitors on the basis of the 3-dimensional structure of PAI-1 and on virtual screening. These compounds have been reported to provide a number of *in vitro* and *in vivo* benefits but none was tested in CNS disease models because of their limited capacity to penetrate the blood-brain barrier (BBB). The existing candidates were therefore optimized to obtain CNS-penetrant compounds. We performed an *in vitro* screening using a model of BBB and were able to identify a novel, low molecular PAI-1 inhibitor, TM5484, with the highest penetration ratio among all other candidates. Next, we tested the effects on inflammation and demyelination in an experimental allergic encephalomyelitis mice model. Results were compared to either fingolimod or 6α-methyl-prednisolone. Oral administration of TM5484 from the onset of signs, ameliorates paralysis, attenuated demyelination, and axonal degeneration in the spinal cord of mice. Furthermore, it modulated the expression of brain-derived neurotrophic factor, which plays a protective role in neurons against various pathological insults, and choline acetyltransferase, a marker of neuronal density. Taken together, these results demonstrate the potential benefits of a novel PAI-1 inhibitor, TM5484, in the treatment of MS.

153

Introduction

Multiple sclerosis (MS), a chronic, inflammatory, demyelinating disease of the central nervous system (CNS), is a leading cause of disability in young, mainly female, adults [1]. Its pathological hallmarks are inflammation and demyelination; they follow the entry of fibrinogen into the CNS, inducing an inflammatory response and axonal damage [2,3].

A link between MS and alterations in the endogenous fibrinolitic system has been identified previously. In particular, increased plasminogen activator inhibitor 1 (PAI-1) levels in the cerebrospinal fluid as well as in acute lesions of patients with MS have been described [4,5]. In the same line of evidence, PAI-1 deficient mice appear to be at least partially protected from chronic relapsing experimental allergic encephalomyelitis (CREAE), a model of MS [6].

Previously, we developed a series of orally active, low molecular PAI-1 inhibitors, relying on virtual screening and the 3-dimentional structure of the complex of PAI-1 with its inhibitory peptide [7]. In addition to their predictable anti-thrombotic effects, these compounds have demonstrated to be valuable in numerous preclinical models, including pulmonary fibrosis, macrophage infiltration, bone marrow regeneration, and arteriosclerosis [7,8,9,10]. However, none of these PAI-1 antagonists have been investigated in CNS diseases models because of their inability to cross the blood brain barrier (BBB). We therefore optimized the existing candidates in order to obtain a drug with CNS-penetrant properties.

Traditionally, a series of physicochemical properties, such as low molecular weight, high lipophilicity (clogP) as well as low polarity (TPSA), are needed to allow effective penetration into the CNS. We selected a class of PAI-1 inhibitors meeting these properties and analyzed their ability to cross the BBB using an *in vitro* model corresponding with the anatomical situation of cerebral microvessels [11]. Eventually, we identified, among all other candidates, a novel, small molecule PAI-1 inhibitor, TM5484, with the highest penetration ratio through the BBB.

We then explored its therapeutic effects on neuroinflammation, demyelination and axonal degeneration, using a mouse model of MS. The effects of the PAI-1 inhibitor were compared with either fingolimod or 6α-methylprednisolone, two drugs currently used to treat patients with MS [12,13]. In addition, we tested the possibility that TM5484 produces neuroprotection through the modulation of the brain-derived neurotrophic factor (BDNF), a member of the neurotrophin family of growth factors known to play a key role in neurons survival, and choline acetyltransferase (ChAT), a marker of neuronal density. A direct link between BDNF and some components of the fibrinolytic pathway has been documented previously [14], but very little is known about PAI-1 and BDNF in MS. Our results indicate that a small molecular PAI-1 inhibitor protects against neuroinflammation, demyelination and axonal degeneration in a mice model of MS, thus validating TM5484 as a potential therapeutic agent.

Materials and Methods

Reagents

Dimethyl sulfoxide (DMSO) was purchased from Nacalai Tesque (Kyoto, Japan), fingolimod (FTY720) from Selleck Chemicals (Houston, TX, USA), and 6α-methylprednisolone, propanolol and verapamil from Sigma Aldrich (Tokyo, Japan).

TM5484 activity and specificity

TM5484 was developed, as a derivative of the PAI-1 inhibitor TM5441 [9], at the United Centers for Advanced Research and Translational Medicine (ART), Tohoku University Graduate School of Medicine, Miyagi, Japan. Its PAI-1 inhibitory activity and specificity were assessed by

154

a chromogenic assay as previously described [7,8]. In brief, the reaction mixture includes 0.15 mol/L NaCl, 50 mmol/L Tris-HCl pH 8, 0.2mmol/L CHAPS, 0.1% PEG-6000, 1% dimethylsulfoxide, 5 nmol/L of either human active PAI-1 (Molecular Innovations, Southfield, MI), human antithrombin III (Sigma-Aldrich, Saint Louis, MO), or human α2-antiplasmin (Sigma-Aldrich), 2 nmol/L of either human 2-chain tPA (American Diagnostica Inc, Stanford, CT), thrombin (Sigma-Aldrich), or plasmin (Sigma-Aldrich), and 0.2 mmol/L of either Spectrozyme tPA (Chromogenix, Milano, Italy), chromogenic substrate S-2238 (Sekisui medical, Tokyo, Japan), or chromogenic substrate S-2251 (Sekisui medical) at a final concentration. Tested compounds were added at various concentrations and the half-maximal inhibition (IC50) was calculated by logit-log analysis. TM5484 inhibited PAI-1 activity with an IC50 value of 3.56 mM but did not inhibit α2-antiplasmin.

TM5484 pharmacokinetics and toxicity

TM5484, suspended in a 0.5% carboxymethyl cellulose sodium salt solution, was administered orally by gavage feeding to male Wistar rats (5 mg/kg; CLEA Japan Inc.). Heparinized blood samples were collected from the vein before (0 h) and 1, 2, 6, and 24 h after oral drug administration. Plasma drug concentration was determined by reverse-phase high-performance liquid chromatography. Maximum drug concentration time (Tmax), maximum drug concentration (Cmax), and drug half-life (T1/2) were calculated as 2h, 22.5 μM and 1.7h, respectively. All toxicity studies followed the International Conference on Harmonization of Technical Requirements for Registration of Pharmaceuticals for Human Use Harmonized Tripartite Guidelines at the non-GLP conditions. A repeated-dose toxicity study of TM5484 (30 mg/kg) was conducted for 2 weeks in 5 Crl:CD (SD) male rats: no adverse effects were observed. TM5484 was negative for the reverse mutation Ames test. The effect of TM5484 on the human ether-a-go-go-related gene (hERG) electric current was investigated in HEL293 cells, transfected with the hERG gene: TM5484 had not effect on hERG electric current.

Analysis of compounds penetration and concentration into CNS

In order to determine the ability of compounds to penetrate into CNS we used an *in vitro* model of BBB (RBT-24H, BBB Kit, PharmaCo-Cell Company Ltd. Nagasaki, Japan). Verapamil and Propanolol were used as a negative and positive control, respectively. This BBB model was reconstructed by the culture of both primary rat brain micro vascular endothelial cells and rat brain pericytes separated by a macroporous Millicell membrane (24 wells, pore size: 3.0 μm, Millipore, Bedford, MA, USA). Briefly, we pre-incubated the BBB kits at 37 °C in 5% CO_2 conditions for 4–5 days, in order to strongly reconstruct the barrier integrity and tight-junctions. To evaluate the barrier integrity and confirm the functionality of the tight-junctions, trans-endothelial electrical resistance (TEER) was measured at day 5-post incubation. Assays were carried out using TEER values in the range of 150-to 300-Ω cm^2 [11]. Once the tight junctions reach a TEER of 300-Ω cm^2, 0.9 mL PBS-based assay medium was added to blank 24-well culture plates. Prior to incubation, selected compounds were diluted in DMSO 100%. The compounds suspended in 0.2 mL assay medium were fortified into the apical side and incubated for 30 min. Next, the medium from both the apical and the basolateral sides were collected and further analyzed by liquid chromatography–mass spectrometry. Transport was measured by detecting the amount of compound from the lower (basal, brain-side) compartment and was calculated using the apparent permeability coefficient (*P*app), a formula provided by PharmaCo-Cell Company Ltd.